

# Turbulence-driven angular momentum transport in modulated Kepler flows

G. RÜDIGER, Potsdam, Germany

Astrophysikalisches Institut Potsdam

A. DRECKER, Potsdam, Germany

Astrophysikalisches Institut Potsdam

Received 2001 May 17; accepted 2001 May

The velocity fluctuations in a spherical shell arising from sinusoidal perturbations of a Keplerian shear flow with a free amplitude parameter  $\varepsilon$  are studied numerically by means of fully 3D nonlinear simulations. The investigations are performed at high Reynolds numbers, i.e.  $3000 < \text{Re} < 5000$ . We find Taylor-Proudman columns of large eddies parallel to the rotation axis for sufficiently strong perturbations. An instability sets in at critical amplitudes with  $\varepsilon_{\text{crit}} \propto \text{Re}^{-1}$ . The whole flow turns out to be almost axisymmetric and nonturbulent exhibiting, however, a very rich radial and latitudinal structure. The Reynolds stress  $\langle u'_r u'_\phi \rangle$  is positive in the entire computational domain, from its Gaussian radial profile a positive viscosity-alpha of about  $10^{-4}$  is derived. The kinetic energy of the turbulent state is dominated by the azimuthal component  $\langle u'^2_\phi \rangle$  whereas the other components are smaller by two orders of magnitude. Our simulations reveal, however, that these structures disappear as soon as the perturbations are switched off. We did not find an “effective” perturbation whose amplitude is such that the disturbance is sustained for large times (cf. Dauchot & Daviaud 1995) which is due to the effective violation of the Rayleigh stability criterion. The fluctuations rapidly smooth the original profile towards to pure Kepler flow which, therefore, proves to be stable in that sense.

*Key words:* Turbulence theory, nonlinear hydrodynamics, angular momentum transport

## 1. Introduction

The reason for the massive transport of angular momentum which enables the formation of the protoplanetary disk is the key question in accretion disk physics. Mostly this mechanism operates at very high Reynolds numbers so that the influence of molecular viscosity is assumed to be negligible. This raises the problem of explaining efficient transport in nearly inviscid flows, which are still a challenge for numerical simulations because of the need for high numerical resolution due to the rich small-scale structure.

It is widely accepted that small-scale turbulence emerging from shear flow instabilities can lead to enhanced *outward* transport – in opposition to the properties of convection phenomena in thin Keplerian disks. For the latter case several *hydrodynamic* computations have revealed an *inwards* transport of angular momentum, i.e. towards the high rotation rates. Ruden et al. (1988) estimated that a modest effective viscosity will result from the largest convective eddies. Ryu & Goodman (1992) started to find negative correlations  $\langle u'_r u'_\phi \rangle$  for convection in Keplerian disks, and Cabot & Pollack (1992) found at low Reynolds numbers that the Reynolds stress can change sign with increasing rotation rate. Kley et al. (1993) derived from their numerical studies that large-scale convective motions can lead to an inward flux of angular momentum. Negative values for the mentioned cross correlation also appear in the simulations of Stone & Balbus (1996) probing the role of vertical convective motions to provide angular momentum transport in a Keplerian disk. In Rüdiger et al. (2001) it is shown that an anisotropy in the form of dominating radial velocity fluctuations

$$\langle u'^2_r \rangle > \langle u'^2_\phi \rangle \tag{1}$$

should be responsible for negative cross correlations and v.v. Anisotropic turbulence fields under the influence of global rotation exhibits extra terms in the cross correlations  $\langle u'_r u'_\phi \rangle$  which do not vanish for rigid rotation (‘ $\Lambda$ -effect’, see Rüdiger 1989). Its sign depends on anisotropies in the turbulence field such as in (1). The question arises whether pure Keplerian shear flow instabilities also fit this concept, although they are known to be linearly stable according to the Rayleigh criterion.

For the solar nebula differential rotation alone has been suggested by Dubrulle (1993) as a possible explanation for the angular momentum transfer. By means of a stability analysis it has been shown that finite but localized

perturbations to the mean shear flow, which can occur due to pressure fluctuations or material impact, could lead to an instability independent of disk properties like temperature, pressure or density.

Such finite amplitude perturbations for shear flows have been investigated numerically mainly in plane Couette flow, which is known to be linearly stable and due to the lack of curvature of the velocity profile the equations which have to be simulated are simplified significantly. Orszag & Kells (1980) have shown that a transition to turbulence at  $\text{Re} = 1250$  requires fully 3D disturbances, but since they have used a rather low numerical resolution ( $16 \times 33 \times 16$ ) they could not simulate the fully developed turbulent state. Finite-amplitude steady-state solutions have been found by Nagata (1990) for  $\text{Re} = 125$ . Lundbladh & Johansson (1991) studied the development of turbulent spots in plane Couette flow for Reynolds numbers between 300 and 1500 by means of direct numerical simulations, and actually they found turbulence to be sustained for sufficiently high Reynolds numbers,  $\text{Re} > 375$ . Corresponding experiments have been performed by Dauchot & Daviaud (1995) for  $\text{Re} < 400$  to determine the critical amplitude  $\varepsilon$  and found a power-law behavior

$$\varepsilon \sim (\text{Re} - \text{Re}_{\text{NL}})^{-\alpha} \quad \text{with } 0.3 < \alpha < 0.8, \quad (2)$$

where  $\text{Re}_{\text{NL}}$  is the nonlinear critical Reynolds number, below which no sustained spots have been observed. This expression, valid only in the neighborhood of  $\text{Re}_{\text{NL}}$ , resembles a transition in terms of critical phenomena. However, for large Reynolds numbers an asymptotic behavior like

$$\varepsilon \sim \text{Re}^{-\beta} \quad (3)$$

holds. The parameter  $\beta$  was shown by Dubrulle & Zahn (1991) to be  $1/3$  for plane Couette flow.

As has been pointed out by Balbus & Hawley (1996) the interaction between the velocity fluctuations and the background mean flow differs fundamentally for cartesian shear-flows and differential rotation. They used inviscid simulations of the Euler equations at moderate resolution of  $64^3$ , but while turbulence was sustained in shear layers they found no numerical evidence that Keplerian flow at high Reynolds numbers is nonlinearly unstable.

For accretion disks this problem now seems to have been solved by the finding that even a pure Keplerian shear flow can be unstable when weak magnetic fields are present (Balbus & Hawley 1991). This magnetic shear flow instability does only operate in magnetically well coupled disks if the magnetic field is neither too weak nor too strong.

In this paper we present results concerning the nonlinear stability of a perturbed Kepler flow for Reynolds numbers in the range  $3000 < \text{Re} < 5000$  obtained by fully nonlinear simulations of the Navier-Stokes equation. First we started with some sinusoidal internal noise perturbing the mean Keplerian shear flow and determined the critical amplitude for a given Reynolds number. In some sense, the modulation of the Kepler flow is used in order to simulate force-driven turbulence. Afterwards, when the kinetic energy has equilibrated, the perturbations have been switched off so that a pure Kepler flow remains. The kinetic energy decays very fast within a small fraction of a viscous time, thus our simulations finally confirm that a Kepler flow is nonlinearly stable even at high Reynolds numbers.

## 2. Mathematical formulation

We focus on the local and global properties of turbulence arising from finite amplitude perturbations. We consider a differentially rotating spherical shell of an incompressible fluid with inner radius  $R_i$  and outer radius  $R_o$ , which enables us to study the large scale structure as well.

The mean flow is assumed to be Keplerian for large radii but perturbed by sinusoidal variations, i.e.

$$\boldsymbol{\Omega} = \Omega_0 \frac{(1 + \varepsilon \sin(2\delta\varpi/\varpi_0))}{\sqrt{1 + (\varpi/\varpi_0)^3}} \mathbf{e}_z, \quad (4)$$

thus we are considering the noise induced by the perturbations as being part of the equilibrium profile (see Fig. 1).

This rotation law depends only on the distance  $\varpi = r \sin \theta$  to the rotation axis, where the parameter  $\varpi_0$  is given by  $\varpi_0 = (R_o - R_i)/2$ . The perturbations we use are characterized by the parameter  $\varepsilon$  describing the amplitude of the fluctuations and the number of periods  $\delta/\pi$  placed in a half shell diameter. This choice of localized perturbations allows for a smooth transition to the unperturbed Keplerian shear flow by decreasing the amplitude  $\varepsilon$ . Because of numerical requirements we have restricted ourselves to  $\delta = 12\pi$  which can give rise to small-scale structures of radial dimensions of  $1/24$ .

According to the Rayleigh criterion a purely Keplerian shear flow is linearly stable with respect to infinitesimal axisymmetric perturbations, however due to fluctuations this stability criterion can be violated locally. It happens locally for all  $\varepsilon$  values exceeding  $0.007$ .<sup>1</sup>

<sup>1</sup>As for finite value of  $\varepsilon$  the basic flow may have a number of inflection points it is also worth to mention Rayleigh's inflection point theorem after which it is a *necessary* condition for instability to infinitesimal disturbances (for parallel shear flows) that an inflection point exists. But there is no claim that any velocity profile with an inflection point is unstable (Acheson 1990).

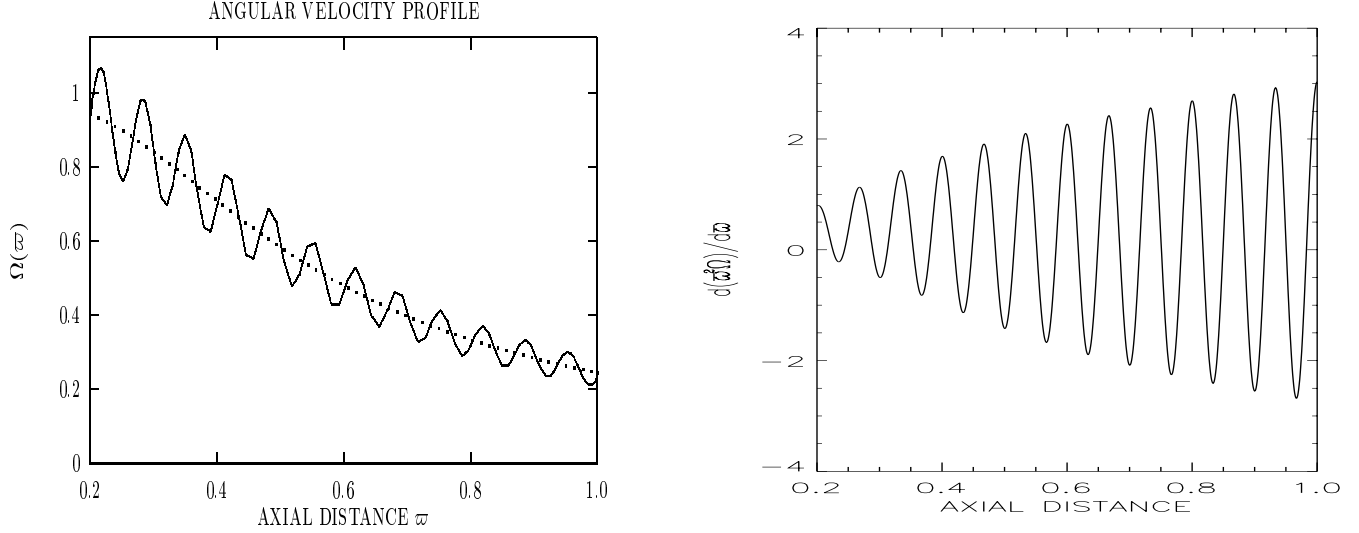


Fig. 1: LEFT: The mean Keplerian shear flow (dotted line,  $\varepsilon = 0$ ) is perturbed by sine-like fluctuations. The full line in the diagram represents the resulting velocity profile for the values  $\varepsilon = 0.125$  and  $\delta = 12\pi$ , the latter corresponding to approximately 12 periods. RIGHT: Negative values indicate local violations of the Rayleigh stability criterion

Since this instability does not depend on the behavior of temperature, pressure and density we do not have to take into account the temperature equation. Moreover, for simplicity we assume the density to be constant throughout the whole shell.

Length and time are normalized with respect to the difference in radii and to the viscous diffusion time  $\tau = (R_o - R_i)^2/\nu$ , i.e.

$$\mathbf{r} = (R_o - R_i)\hat{\mathbf{r}}, \quad t = \frac{(R_o - R_i)^2}{\nu}\hat{t}. \quad (5)$$

Then the velocity field is normalized by the rate  $\Omega_0$  of the prescribed differential rotation,

$$\mathbf{u} = (R_o - R_i)\Omega_0\hat{\mathbf{u}}. \quad (6)$$

Expressed in terms of these variables the Navier-Stokes equation for the fluctuations  $\mathbf{u}' = \mathbf{u} - \mathbf{u}_0$  becomes

$$\frac{\partial \mathbf{u}'}{\partial t} - \Delta \mathbf{u}' = -\text{grad } p + \text{Re}(\mathbf{u}' \times \text{rot } \mathbf{u}' + \mathbf{u}_0 \times \text{rot } \mathbf{u}' + \mathbf{u}' \times \text{rot } \mathbf{u}_0) \quad (7)$$

(the hats are now omitted) with the Reynolds number

$$\text{Re} = \frac{\Omega_0(R_o - R_i)^2}{\nu}. \quad (8)$$

Since the vector  $\mathbf{u}$  is divergence-free it can be represented by toroidal and poloidal components (Chandrasekhar 1961)

$$\mathbf{u}' = \mathbf{r} \times \text{grad}\left(\frac{\Phi}{r}\right) + \text{rot}\left(\mathbf{r} \times \text{grad}\left(\frac{\Psi}{r}\right)\right). \quad (9)$$

We consider stress-free boundary conditions for the flow. Thus the cross-components  $\pi_{r\phi}$ ,  $\pi_{r\theta}$  of the viscous stress-tensor  $\pi_{ij} = -\rho\nu(u'_{i,j} + u'_{j,i})$  have to vanish, which can be expressed by the scalar potentials  $\Psi$  and  $\Phi$  as

$$\frac{2}{r} \frac{\partial \Psi_{lm}}{\partial r} - \frac{\partial^2 \Psi_{lm}}{\partial^2 r} = 0, \quad \frac{\partial}{\partial r} \left( \frac{\Phi_{lm}}{r^2} \right) = 0. \quad (10)$$

No normal flow is allowed at  $r = r_i, r_o$  hence the potential  $\Psi$  vanishes at the boundary,

$$\Psi_{lm} = 0. \quad (11)$$

### 3. Numerics

The numerical simulations have been performed by the hydrodynamical part of the spectral magneto-convection code which is described in full detail in Hollerbach (2000). The spectral expansion uses spherical harmonics on the 2-sphere and Chebyshev polynomials in the radial direction

$$\Psi = \sum_{k,l,m} \Psi(k,l,m) T_{k-1}(x) P_l^{|m|}(\cos\theta) e^{im\phi} \quad (12)$$

with the radius  $r$  mapped to the interval  $[-1, 1]$  via

$$r = \frac{r_o + r_i}{2} + \frac{r_o - r_i}{2} x. \quad (13)$$

The radius ratio has been fixed to  $1/5$  throughout while setting the shell diameter to unity:  $r_o - r_i = 1$ . In all diagrams with a radial dependence we show plots versus the ratio  $r/r_o$ , normalizing the outer radius to unity.

The diffusive terms in combination with the boundary conditions are treated implicitly in spectral space, whereas the nonlinear terms are evaluated explicitly on a grid of collocation points. The timestepping is performed by a modified second order Runge-Kutta scheme: first a predictor step calculates an estimated value, and afterwards the resulting spectral coefficients are used for evaluating again the velocity field, which yields a corrected value in a second step.

Because of memory requirements we had to run these simulations on a Convex HPP-1200, where a single time step for a numerical resolution of 40 Chebyshev-, 70 Legendre polynomials and 3 Fourier modes required approximately 5 seconds of CPU time. At Reynolds numbers of  $\text{Re} = 3000 - 5000$  the code runs stably with a time-step of  $3 \times 10^{-5}$ . Thus a run simulating the flow over a period of half a viscous time can be performed within one day of CPU time. In order to avoid aliasing effects when transforming from real space to spectral space and vv. we used a collocation grid of the following dimension:  $\dim(r_i, \theta_j, \phi_k) = 80 \times 105 \times 5$ .

### 4. Results and discussion

We have run simulations in the range  $\text{Re} = 3000 - 5000$  with different values for the amplitude  $\varepsilon$  so that the corresponding minimum perturbation can be determined. A single run where the instability leads to a nondecaying state is discussed in full detail in the following subsection.

#### 4.1. The exemplary case $\text{Re} = 3500$

Figure 2 shows the temporal evolution of the total kinetic energy for a run with  $\text{Re} = 3500$  and several amplitudes  $\varepsilon = 0.1, 0.125, 0.15$  starting from arbitrary initial fields. For  $\varepsilon = 0.15$  the solution grows by one order of magnitude during a time of about 10% of a viscous time after which a turbulent state has been reached. The largest contribution to the kinetic energy is due to the azimuthal component, whereas the radial and meridional components yield contributions which are both smaller by almost two orders of magnitude. A perturbation with  $\varepsilon = 0.125$  still leads to a turbulent configuration, but it is close to the critical amplitude since the kinetic energy decays for  $\varepsilon = 0.1$ .

Figure 3 demonstrates the dominant role of the azimuthal velocity fluctuations in the small-scale flow-pattern. The turbulence field is highly anisotropic with a massive ‘‘Austausch’’ in the  $\phi$ -direction. As already stressed by Biermann (1951) such a flow field contributes to a positive correlation  $\langle u_r u_\phi \rangle$  under the influence of basic rotation (cf. Rüdiger 1989, p. 254) – in contrast to convective patterns, where negative correlations do appear.

As the next step we discuss the spectral distribution of energy. The resulting flow pattern is nearly axisymmetric and steady, higher modes are suppressed by several orders of magnitude:  $E_0 : E_1 : E_2 = 1 : 10^{-2} : 10^{-4}$ . Simulations with higher azimuthal resolution lead to the same quantitative result. For stronger amplitudes  $\varepsilon$  the non-axisymmetric modes become much stronger, but in addition to the numerical difficulties that we encountered in simulating those flows such strong perturbations seem to be physically irrelevant.

The Chebyshev spectrum (Fig. 4) behaves like  $k^{-5}$  for small  $k$  and shows strong peaks at  $k_1 = 1$  and  $k_2 = 22$ , the former corresponding to the global torus-like structure of the flow. The latter peak determines the radial dimension of the turbulence elements  $\ell_{\text{corr}} \simeq 1/k_2 = 0.045$ .

As can be seen from the energy spectrum for the Legendre polynomials the flow is symmetric with respect to the equatorial plane. In general, even  $l$ -modes are stronger by one order of magnitude with a maximum at  $l = 46$  in comparison with odd modes resulting in a total parity of 0.98. The flow is mainly confined to the region  $0.4 < \varpi < 0.8$  where the eddies form Taylor columns. The alignment which is to be expected for high Taylor

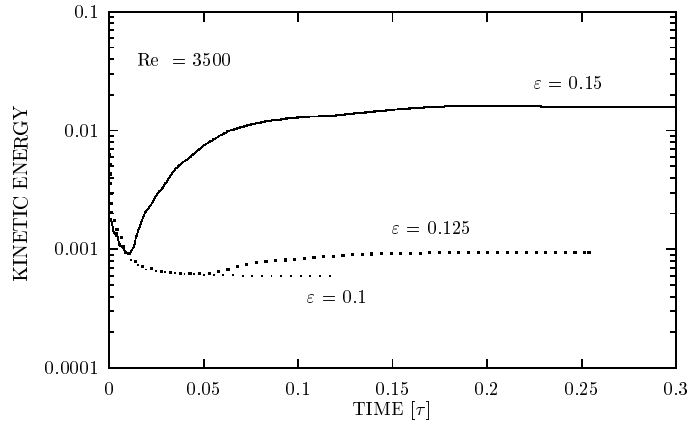


Fig. 2: The kinetic energy reaches a turbulent equilibrium for  $\varepsilon = 0.15, 0.125$ , but decays for  $\varepsilon = 0.1$ . The case  $\varepsilon = 0.125$  is close to the critical amplitude. Time is measured in units of the viscous time.

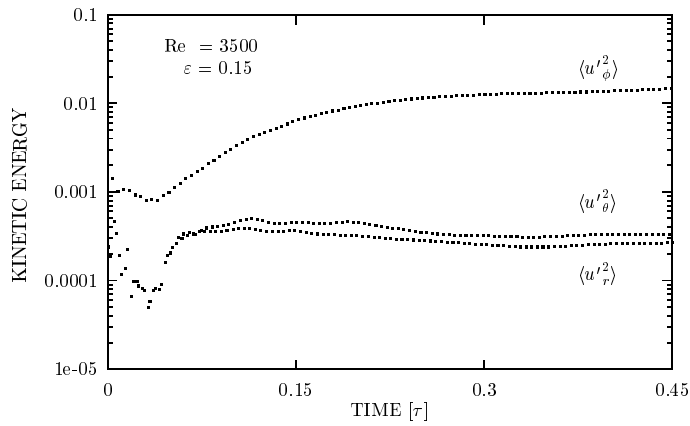


Fig. 3: The kinetic energy of the turbulent state is dominated by the azimuthal component, whereas the other components are smaller by two orders.

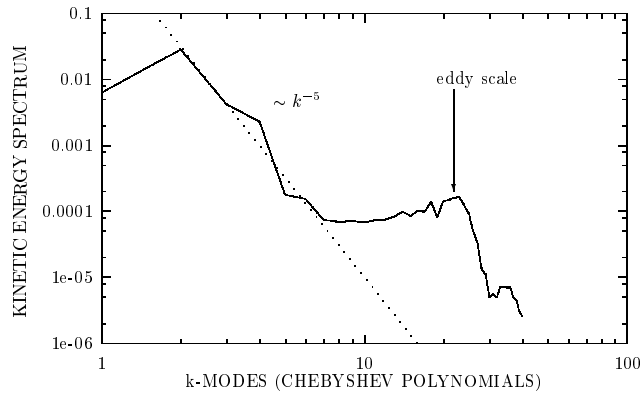


Fig. 4: The Chebyshev spectrum of the kinetic energy for  $Re = 3500$  and  $\varepsilon = 0.15$  decreases like  $k^{-5}$  for large modes. The peak at  $k = 22$  corresponds to the radial dimension  $\ell_{\text{corr}} = 0.045$  of a single eddy.

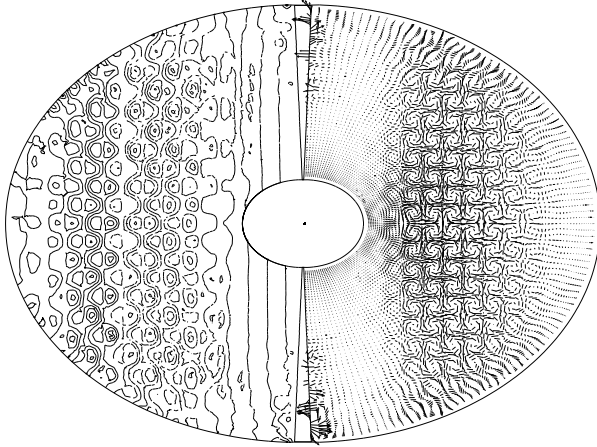


Fig. 5: Left: Contour plot of the azimuthal velocity component. Right: Meridional structure of the velocity field.  $Re = 3500$ ,  $\varepsilon = 0.15$ . The eddies form Taylor-Proudman columns in the range  $0.4 < \varpi < 0.8$ .

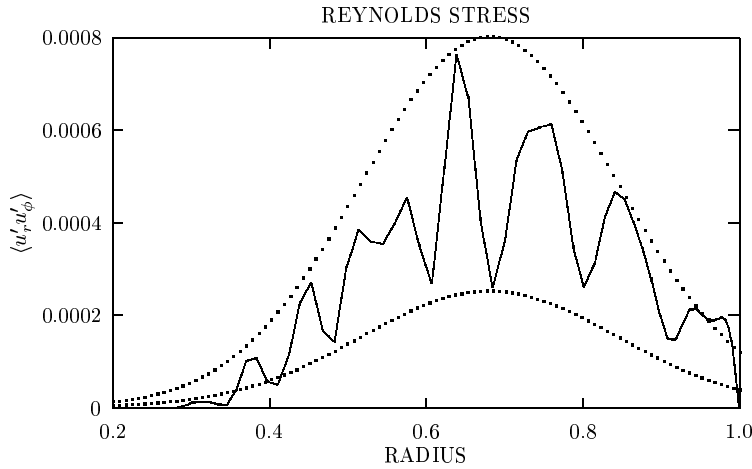


Fig. 6: The cross correlation of the velocity field has a Gauss-type structure in radius. The dotted lines show analytical curves  $\exp -(\varpi - \varpi_0)^2 / (2\sigma^2)$  used for fitting the minima and maxima:  $\varpi_0 \approx 0.68$ ,  $\sigma \approx 0.204$ .  $\varepsilon = 0.15$ ,  $Re = 3500$ .

numbers can also be seen from the contour plot of the radial flow component. We find 9 eddies in the radial and up to 18 eddies in the vertical direction depending on the height of the shell (Fig. 5).

Despite the fact that the total flow looks rather inhomogeneous from a global point of view we make some rough estimates for its eddy viscosity which will agree approximately with the viscosity derived later on. From dimensional analysis one is led to

$$\frac{\nu_T}{\nu} = u_T \cdot \ell_{\text{corr}}, \quad (14)$$

where  $\ell_{\text{corr}}$  and  $u_T$  denote a characteristic radial dimension and velocity. If we insert in this relation a typical eddy velocity and the shell diameter we end up with a rather small value of  $\nu_T/\nu \approx 0.03$ .

Now we turn to the angular momentum transport which is regulated by the dissipative stress. Figure 6 shows the Reynolds stress  $\langle u'_r u'_\phi \rangle$  as a function of the radius calculated by integrating over the 2-sphere for the amplitude  $\varepsilon = 0.15$ . Strong correlation of the velocity field can be found only in the region  $0.5 < r < 0.9$ , the fluctuations being exponentially damped outside, but they are positive in the entire computational domain. Indeed after Fig. 7 there is no exception from the dominance of  $\langle u'^2_\phi \rangle$  in striking difference to relation (1) valid for convective Kepler disks.

The maxima and minima are forming a Gaussian,

$$\text{extremum} \langle u'_r u'_\phi \rangle \propto \exp(-12(r - 0.68)^2), \quad (15)$$

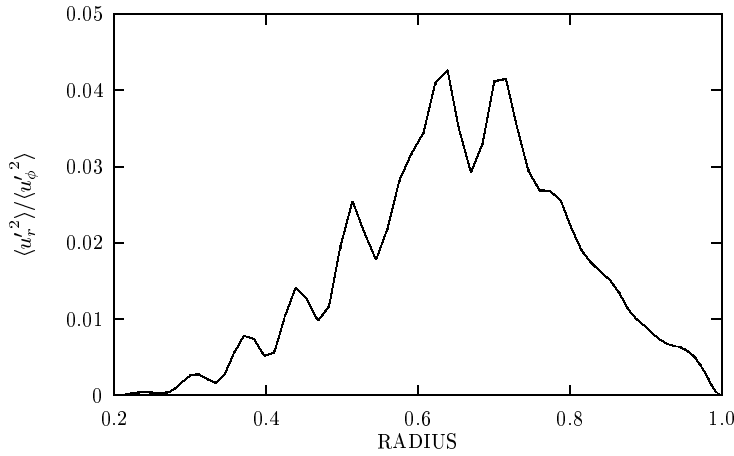


Fig. 7: The intensity ratio in the small-scale flow pattern of the model corresponding to Fig. 6. The azimuthal perturbations dominate the radial ones everywhere in opposition to the condition (1) valid for convection.

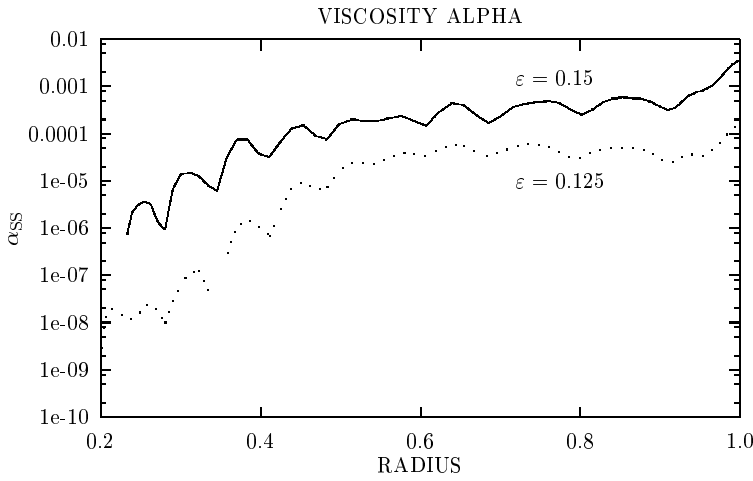


Fig. 8: The viscosity  $\alpha_{SS}$  is positive and nearly constant between  $0.5 < r < 0.9$ . The value of  $\alpha_{SS}$  differs by one order for the amplitudes  $\varepsilon = 0.15$  and  $\varepsilon = 0.125$ .

with a standard deviation of about  $\sigma \approx 0.204$ . We proceed to derive the eddy viscosity  $\nu_T$  by integrating (15) with respect to the radius and normalizing it with the unperturbed Keplerian shear flow  $\Omega_{Kep}$ :

$$\frac{\nu_T}{\nu} \varpi \left( \frac{d\Omega_{Kep}}{d\varpi} \right) = -\text{Re} \langle u_r' u_\phi' \rangle. \quad (16)$$

This prescription yields in the case  $\text{Re} = 3500$  for the ratio of turbulent and molecular viscosity  $\nu_T/\nu = 0.15$ . This turbulent viscosity will now be related to the characteristic length and velocity. Shakura & Sunyaev (1973) have introduced a viscosity alpha using the scale height  $H(\varpi) = \sqrt{r_o^2 - \varpi^2}$ . All uncertainties about the turbulence has been put into this single parameter which allows to construct a variety of  $\alpha$ -type models in accretion disk theory,

$$\nu_T = \alpha_{SS} \Omega_{Kep} H^2. \quad (17)$$

The resulting radial structure for  $\alpha_{SS}$  is shown in Fig. 8 for  $\varepsilon = 0.15$  and  $\varepsilon = 0.125$ . It is positive everywhere. A complete volume integration yields the value  $\alpha_{SS} = 3.75 \times 10^{-4}$ . In the “turbulent” region  $0.5 < r < 0.9$  the viscosity alpha is nearly constant, while the value for  $\varepsilon = 0.125$  is by one order smaller than for  $\varepsilon = 0.15$ . Those low values for all viscosity parameters indicate that we have not found a truly turbulent state, which is confirmed by the fact that the velocity field is stationary. In the next section we study the question whether this state can be sustained for a purely Keplerian rotation law.

#### 4.2. Perturbations as initial fields

After the Rayleigh criterion a pure Keplerian shear flow is stable against axisymmetric, infinitesimal perturbations, but it does not make predictions about the stability of finite amplitude perturbations. In order to check whether

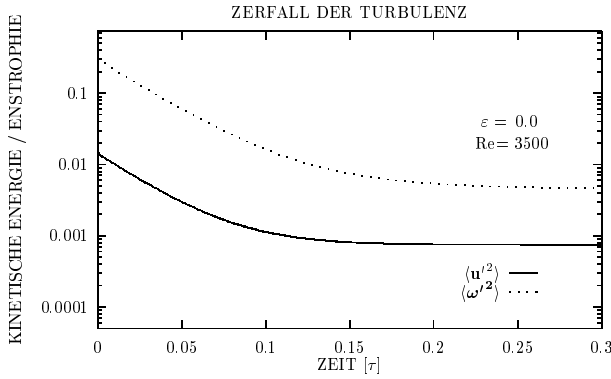


Fig. 9: The kinetic energy  $\langle \mathbf{u}'^2 \rangle$  and the enstrophy  $\langle \boldsymbol{\omega}'^2 \rangle$  decay exponentially within  $t = 0.1 \tau$  as soon as the perturbations  $\varepsilon$  are switched off.

the nonlinear turbulent state discussed in the foregoing subsection can give rise to such a nonlinear instability the resulting flow was used as initial field for a simulation when the perturbations have been switched off, i.e.  $\varepsilon = 0$ . Notice that the initial state contains weak non-axisymmetric contributions.

It turns out that the kinetic energy  $\langle \mathbf{u}'^2 \rangle$  and the enstrophy  $\langle \boldsymbol{\omega}'^2 \rangle$  decay exponentially very fast within a time of 0.15 diffusion times,  $\tau$ , corresponding to approximately 525 orbits (Fig. 9). Within a few orbits the eddy viscosity decreases strongly since the rotational support from the sinusoidal perturbations is missing. After this short period it has reached approximately the value predicted by our estimate of the foregoing section using dimensional analysis:  $\nu_T/\nu \approx 0.02$ . Then it decays like  $\nu_T/\nu \sim e^{-27t/\tau}$ .

Both the enstrophy and the energy dissipation rate  $d\langle \mathbf{u}'^2 \rangle/dt$  are used for a comparison with the decay of homogeneous turbulence by rewriting the energy balance equation

$$\frac{\nu_{\text{eff}}}{\nu} = -\frac{1}{2} \frac{d\langle \mathbf{u}'^2 \rangle}{\langle \boldsymbol{\omega}'^2 \rangle}, \quad (18)$$

where  $\nu_{\text{eff}}$  accounts for the effective nonlinear contributions stemming from the energy flux and for the energy injection by the forced differential rotation. As long as the flow shows strong local inhomogeneities this value remains nearly constant, but after  $t = 0.1 \tau$ , when the flow consists of several almost homogeneous domains, an exponential decay like  $\nu_{\text{eff}}/\nu \sim e^{-33t/\tau}$  sets in. Hence, the turbulence does not survive the transition to a pure, undisturbed Kepler flow.

## 5. Summary and conclusions

The results for runs with several Reynolds numbers and with different perturbation amplitudes are summarized in Table 1 starting with  $Re = 3000$ .

Since for stress-free boundary conditions the angular momentum is conserved, the kinetic energy does not decay to zero completely even for a purely Keplerian shear flow if the initial fields contain nonvanishing angular momentum. Therefore we started our series of runs at  $Re = 3000$  without any perturbation. A calculation of the angular momentum yielded  $L_z \approx -5.4 \times 10^{-2}$  in this case. We are considering the corresponding kinetic energy  $E_{\text{kin}} \approx -5.89 \times 10^{-4}$  as an offset for the subsequent runs with perturbations to the velocity profile  $\varepsilon \neq 0$  rather than performing a transformation such that  $L_z = 0$ .

The minimum value of the perturbation amplitude for reaching a turbulent state at  $Re = 3000$  turned out to be  $\varepsilon = 0.15$ . The corresponding kinetic energy exceeded the energy offset due to initial angular momentum just a little bit, thus indicating that this case is close to neutral stability. The eddy viscosity accepted already a steady finite value of order  $10^{-2}$  while the viscosity  $\alpha$  reached approximately  $10^{-5}$ . Increasing the amplitude to  $\varepsilon = 0.175$  all values grow by approximately one order of magnitude. Even for strong perturbations we never find a viscosity  $\alpha$  larger than  $10^{-4}$  indicating, therefore, no efficient mechanism of angular momentum transport in this model. The kinetic energy has been vastly dominated in all runs by the azimuthal component throughout.

The onset of turbulence is mainly governed by the Reynolds number, for which one usually assumes that the critical amplitude behaves according to a power law like  $\varepsilon_{\text{crit}} \sim Re^{-\beta}$ . For plane Couette flow an analytical treatment by Dubrulle & Zahn (1991) yielded for this parameter  $\beta = 1/3$ .

Using the critical amplitudes which we have determined in our runs we find roughly the following scaling

$$\varepsilon_{\text{crit}} \sim Re^{-1}. \quad (19)$$

Table 1: The total kinetic energy, the eddy viscosity and the viscosity alpha for several combinations of Reynolds numbers and perturbation amplitudes.

Re	$\varepsilon$	$\langle \mathbf{u}^2 \rangle$	$\nu_T/\nu$	$\alpha_{SS}$
3000	0.0	$5.89 \times 10^{-4}$	$\approx 10^{-5}$	$\approx 10^{-8}$
	0.125	$5.97 \times 10^{-4}$	$\approx 10^{-5}$	$\approx 10^{-8}$
	0.15	$7.34 \times 10^{-4}$	$9.45 \times 10^{-3}$	$1.25 \times 10^{-5}$
	0.175	$8.55 \times 10^{-3}$	$1.03 \times 10^{-1}$	$1.84 \times 10^{-4}$
3500	0.1	$5.95 \times 10^{-4}$	$\approx 10^{-5}$	$\approx 10^{-8}$
	0.125	$9.37 \times 10^{-4}$	$1.72 \times 10^{-2}$	$2.75 \times 10^{-5}$
	0.15	$1.56 \times 10^{-2}$	$1.50 \times 10^{-1}$	$3.75 \times 10^{-4}$
4000	0.1	$5.85 \times 10^{-4}$	$\approx 10^{-5}$	$\approx 10^{-8}$
	0.11	$1.73 \times 10^{-3}$	$3.70 \times 10^{-2}$	$6.63 \times 10^{-5}$
5000	0.075	$5.74 \times 10^{-4}$	$\approx 10^{-6}$	$\approx 10^{-9}$
	0.085	$1.72 \times 10^{-3}$	$4.2 \times 10^{-2}$	$7.52 \times 10^{-5}$
	0.09	$3.84 \times 10^{-3}$	$7.71 \times 10^{-2}$	$1.53 \times 10^{-4}$

This behaviour predicts that the instability will set in at high Reynolds numbers already for weak perturbations, but as our simulations have shown the nonaxisymmetric modes (being necessary for the occurrence of true turbulence) will be excited only for fairly strong perturbations. Accordingly, the turbulence was not sustained when the perturbations have been switched off, instead the eddy structures decayed very fast. Thus, our studies give no indications that Kepler rotation is nonlinearly unstable against finite amplitude perturbations (for Reynolds numbers up to  $10^3$ ).

## References

- Acheson, D.J.: 1990, *Elementary Fluid Dynamics*, Clarendon, Oxford
- Balbus, S. A., Hawley, F.: 1991, *ApJ* 376, 214
- Balbus, S. A., Hawley, F., Stone, J. M.: 1996, *ApJ* 467, 76
- Biermann, L.: 1951, *Z. Astrophysik* 28, 304
- Cabot, W., Pollack, J. R.: 1992, *Geophys. Astrophys. Fluid Dyn.* 64, 97
- Chandrasekhar, S.: 1961, *Hydrodynamic and Hydromagnetic Stability*, Clarendon, Oxford
- Dauchot, O., Daviaud F.: 1995, *Phys. Fluids* 7, 901
- Dauchot, O., Daviaud F.: 1995, *Phys. Fluids* 7, 335
- Dubrulle, B., Zahn J.-P.: 1991, *J. Fluid Mech.* 231, 561
- Dubrulle, B.: 1993, *Icarus* 106, 59
- Hollerbach, R.: 2000, *Int. J. Num. Meth. Fluids* 32, 773
- Kley, W., Papaloizou, J. C. B., Lin, D. N.: 1993, *ApJ* 416, 679
- Lundbladh, A., Johansson, A. V.: 1991, *J. Fluid Mech.* 229, 499
- Nagata, T.: 1990, *ApJ* 376, 214
- Orszag, S. A., Kells, L. C.: 1980, *J. Fluid Mech.* 96, 159
- Ruden, S. P., Papaloizou, J. C. B., Lin, D. N. C.: 1988, *ApJ* 329, 739
- Rüdiger, G.: 1989, *Differential rotation and stellar convection: Sun and solar-type stars*, Gordon and Breach, Science Publishers
- Rüdiger, G., Tschäpe, R., Kitchatinov, L.L.: 2001, *MNRAS* (subm.)
- Ryu, D., Goodman, J.: 1992, *ApJ* 388, 438
- Shakura, N. I., Sunyaev, R. A.: 1973, *A&A* 24, 337
- Stone, J. M., Balbus, S. A.: 1996, *ApJ* 464, 364

Addresses of the authors:

Günther Rüdiger, Astrophysikalisches Institut Potsdam, An der Sternwarte 16, D-14482 Potsdam, Germany, e-mail: GRuediger@aip.de

Andreas Drecker, Astrophysikalisches Institut Potsdam, An der Sternwarte 16, D-14482 Potsdam, Germany